

STATE GRAPHS AND FIBERED STATE SURFACES

DARLAN GIRÃO AND JESSICA PURCELL

ABSTRACT. Associated to every state surface for a knot or link is a state graph, which embeds as a spine of the state surface. A state graph can be decomposed along cut-vertices into graphs with induced planar embeddings. Associated with each such planar graph is a checkerboard surface, and each state surface is a fiber if and only if all of its associated checkerboard surfaces are fibers. We give an algebraic condition that characterizes which checkerboard surfaces are fibers directly from their state graphs. We use this to classify fibering of checkerboard surfaces for several families of planar graphs, including those associated with 2-bridge links. This characterizes fibering for many families of state surfaces.

1. INTRODUCTION

Associated to a diagram of a knot or link in the 3-sphere are several embedded spanning surfaces called *state surfaces*. These arise from a choice of Kauffman state, which were introduced by Kauffman to give insight into the Jones polynomial [21]. The associated surfaces, introduced in [26] and [27], arise naturally as ribbon graphs. State surfaces are known to be related to knot and link polynomials; see for example [4, 7, 18]. State surfaces are also related to the hyperbolic geometry of the link complement for hyperbolic links; see for example [1, 2, 5, 7, 8, 9]. Because of their connections with geometry, topology, and link invariants, these surfaces have recently become objects of much study in knot theory. In this paper, we consider when such surfaces can be fibers.

If we put restrictions on the Kauffman states, there are already results that determine if a state surface is a fiber. For a class of states called homogeneously adequate states, work of Futer [6] and Futer, Kalfagianni, and Purcell [7] shows that the associated state surface is a fiber if and only if a related graph, called the reduced state graph, is a tree. This answered a question of Ozawa [26]. In [7], it is shown that for some special states, fibering is also indicated immediately by the colored Jones polynomial. For other restrictions of state surfaces, the problem of fibering such state surfaces has been considered by Girão [12] and Girão, Nogueira, and Salgueiro [13]. However, we wish to find ways of classifying fibrations of *all* state surfaces, without restrictions on the Kaufmann state.

The study of fibered knots and links has been ongoing since the early 1960s, introduced by work of Neuwirth [24] and Stallings [29], followed by results of Murasugi [22]. In the 1970s, further work of Stallings [30] and Harer [15] gave insight on constructing fibered knots and links. In the 1980s, Gabai [10] gave a procedure to decide whether an oriented link is fibered, and this has had numerous applications. To date, several results exist that prove that a given knot is fibered. For example, work of Ghiggini [11] and Ni [25] shows that whether or not a knot is fibered can be determined using knot Floer homology. However, we are interested not in whether there exists some fibering of a knot or link, but whether a particular fixed state surface is a fiber. This is not always easily determined even if it is known that a link is fibered; see the discussion below on 2-bridge knots and links.

There do exist examples of knots and links and fixed surfaces for which fibering can be determined immediately from a diagram. These include standard diagrams of pretzel links, due to Gabai [10], and Montesinos knots, due to Hirasawa and Murasugi [17]. Previous results on fibering of state surfaces for restricted states are also along these lines [6, 7, 12, 13]. These are the types of results that we wish to generalize.

The first main result of this paper is Theorem 2.5, which says that whether a state surface is a fiber is completely determined by an associated graph G_σ , called the state graph, which can be quickly read from the diagram. In particular, we reduce the problem of determining fibering for a state surface with a complicated embedding into S^3 to the problem of determining fibering for checkerboard state surfaces.

The next main result is Theorem 4.2, which gives an algebraic condition that characterizes when a checkerboard state surface is a fiber. In particular, it suffices to prove that a homomorphism $\phi: \pi_1(G_\sigma) \rightarrow \pi_1(S^3 - G_\sigma)$ is an isomorphism, where the map ϕ is read directly from G_σ ; see Proposition 4.5. Stallings gave a method to determine whether a homomorphism of free groups is an isomorphism, now called the Stallings folding algorithm [31]. This has had many applications, especially in geometric group theory. By work of Touikan, the algorithm produced runs in almost linear time [32]. We show here that our state graph homomorphisms feed neatly into the Stallings folding algorithm, and thus we can read whether or not a state surface is a fiber from its state graph in almost linear time.

We conclude the paper by giving several applications, determining many new examples of families of knots and links with fibered state surfaces. One additional result that comes out of this work, which may be of independent interest, is a classification of those 2-bridge link diagrams for which the (bounded) checkerboard surface is a fiber. Recall that a 2-bridge link is determined by a rational number p/q , and the link has several natural diagrams, determined by different continued fraction expansions of $p/q = [a_{n-1}, \dots, a_1]$ (notation described in Section 5). Denote the diagram by $K[a_{n-1}, \dots, a_1]$. Hatcher and Thurston note that a 2-bridge knot is fibered if and only if it is isotopic to $K[\pm 2, \dots, \pm 2]$, and the fiber is isotopic to a particular spanning surface [16]. However, the surfaces they describe do not ever have the form of a checkerboard surface. Here, we determine exactly which values of a_{n-1}, \dots, a_1 give a checkerboard surface that is a fiber, i.e. isotopic to one of Hatcher and Thurston's fibered surfaces.

1.1. Organization. In Section 2, we review terminology used in this paper. In particular, we define Kauffman states, state surfaces, and state graphs. With terminology defined, we then state carefully our first result, Theorem 2.5. In Section 3, we review important theorems on fibering due to Gabai and others, and give the proof of Theorem 2.5. In Section 4, the statement and proof of our algebraic characterization of fibering is given, after recalling work of Stallings. Applications are then presented in Section 5. This section includes, for example, a complete characterization of when the bounded checkerboard surfaces of 2-bridge links are fibered, Theorem 5.7.

1.2. Acknowledgements. We thank João Nogueira for helpful conversations, and we thank David Futer for bringing our attention to Stallings folds. The first author was partially supported by Conselho Nacional de Desenvolvimento Científico e Tecnológico (CNPq) grants 446307/2014–9 and 306322/2015–3 and the CAPES Foundation. The second author was partially supported by the Australian Research Council.

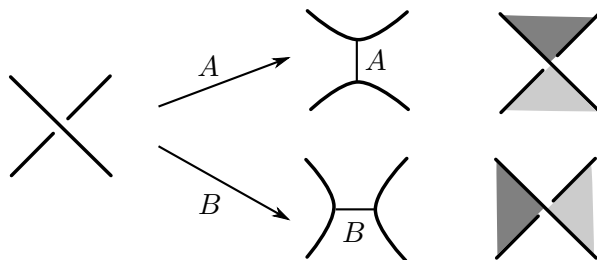


FIGURE 1. The two choices of resolutions for the split of a crossing.

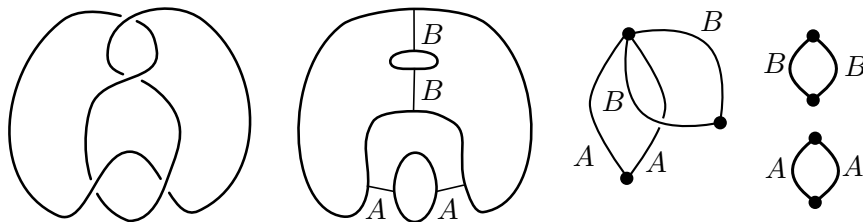


FIGURE 2. Left to right: A diagram, a Kauffman state, the corresponding state graph with its associated embedding, and the decomposition along cut-vertices into planar graphs.

1.3. Dedication. While this work was underway, the first author, Darlan Girão, was diagnosed with aggressive cancer, and he died before the paper was complete. Darlan was a wonderful colleague and friend, and he will be missed. This paper is dedicated to his memory.

2. PRELIMINARIES AND MAIN RESULTS

Given a diagram $D(K)$ of a link K , at each crossing there are two choices of *resolutions* for the smoothing of the crossing: an A -resolution or a B -resolution; see Figure 1. By choosing a resolution at each crossing, we construct a collection of circles, called *state circles*, which are the boundaries of disjoint disks, called *state disks*. These state circles induce a decomposition of the plane into connected components that we call *regions*. Connect the circles by edges labeled A or B , to indicate a resolved crossing and its resolution, as in Figure 1.

A *Kauffman state* σ of a link diagram $D(K)$ is a choice of resolution at each crossing of $D(K)$. Given a state σ , add twisted bands connecting the state disks, one for each crossing, according to the choice of resolution. We thus obtain a surface whose boundary is the link K . The resulting surface S_σ is called the *state surface* of σ . For example, the Seifert surface of an oriented diagram of a link is a particular case of a state surface, where the resolution of each crossing is defined by the orientation of the link components.

The *state graph* G_σ has one vertex for each state disk and one edge for each band defined by the state σ . We label the edges by A or B according to the resolution of the respective crossings. Note that the graph G_σ has a natural embedding in the surface S_σ as its spine. Figure 2 shows an example of a diagram, a Kauffman state, and the corresponding state graph with its associated embedding.

Definition 2.1. We say that a vertex v *decomposes* a graph G into components G_1, G_2 if G_1 and G_2 contain at least one edge, and $G = G_1 \cup G_2$ and $G_1 \cap G_2 = \{v\}$. We also say v is a *cut-vertex* of G .

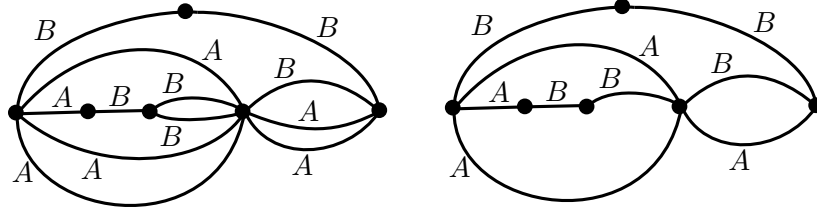


FIGURE 3. On the left is a 2-connected state graph with a fixed planar embedding. On the right is the associated reduced state graph.

Lemma 2.2. *The cut-vertices of a state graph decompose it into a finite collection of planar 2-connected graphs, with planar embeddings determined by the Kauffman state.*

This decomposition is illustrated for the example of Figure 2 on the far right of that figure.

It is not hard to see that every state graph admits a planar embedding. However, this embedding may not be isotopic to the embedding associated with the state surface, and so it is not obviously useful from the point of view of analyzing spanning surfaces. The point of Lemma 2.2 is that after decomposing along cut-vertices, the remaining pieces all have a planar embedding induced from the state surface.

Proof of Lemma 2.2. Suppose each state circle bounds a disk that is disjoint from the diagram of the link; for example this will hold if the state graph has no cut-vertices. The Kauffman state connects these disks by edges labeled A or B that lie in the plane, and are disjoint from the interiors of the disks. Thus when we collapse each disk to a point, the state graph we obtain remains planar.

So suppose there is a state circle such that disks on both sides meet the diagram. Then this corresponds to a cut-vertex. There must be an innermost such state circle C . That is, C bounds a disk D in the plane S^2 such that both D and $S^2 - D$ meet the diagram, but all state circles within D bound disks disjoint from the diagram. Decompose the state graph along the corresponding cut-vertex. This decomposes the state graph into a graph associated with the outside of D and a graph associated with the inside of D . On the outside of D , there are at most $n - 1$ cut-vertices, and so the result follows by induction. On the inside of D , all state circles bound disks disjoint from the diagram. But now the state circle C also bounds a disk $D' = S^2 - D$ disjoint from the remainder of the diagram. By the previous argument, the graph we obtain by collapsing all these disks to points is planar, with embedding determined by the Kauffman state. \square

As in Figure 2, the planar graphs determined by Lemma 2.2 may have multiple edges connecting the same pair of vertices, and these edges may be labeled both A and B . We say that two edges are *parallel within the plane* if the edges are ambient isotopic in the plane in the complement of all other edges and vertices of the graph.

For multiple edges connecting the same pair of vertices that have the same label (A or B) and that are parallel within the plane, remove all but one such edge. When all such edges are removed, the resulting graph is called the *reduced state graph*. Note that multiple edges may remain in the reduced state graph, but they will either have distinct labels, or they will not be parallel. Figure 3 illustrates this by example.

Any planar graph with edges labeled A and B corresponds to a *checkerboard surface* as follows. For each vertex, take a disk. For each edge, take a twisted band, with direction of twisting determined by the label A or B ; see Figure 4.

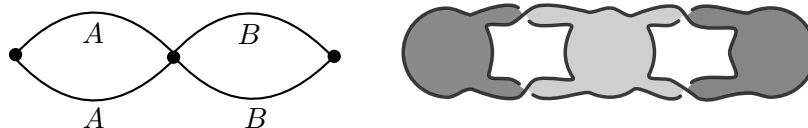


FIGURE 4. A planar graph with edges labeled A and B corresponds to a checkerboard surface.

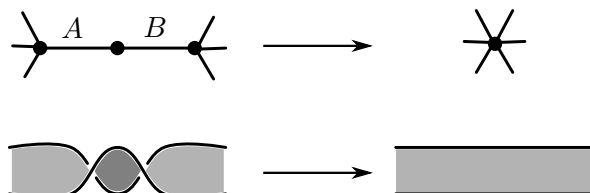


FIGURE 5. Collapsing consecutive edges with distinct labels.

In addition to multiple edges, we may also reduce our planar state graphs by considering consecutive edges.

Definition 2.3. Two edges are called *consecutive* if they share a vertex v and there are no other edges incident at v .

Lemma 2.4. *If two consecutive edges in a reduced state graph do not have the same label, then the corresponding link and state surface can be isotoped to a simpler link, removing two crossings. On the graph, this corresponds to collapsing the two edges.*

Proof. The simplification is shown in figure 5. □

We can now state our first main theorem.

Theorem 2.5. *Let K be a diagram of a link in S^3 with oriented state surface S_σ associated to the state σ . Decompose the corresponding state graph G_σ along cut-vertices into planar graphs, and consider the reduced planar graph, with parallel edges with the same label removed. Finally, collapse consecutive edges with distinct labels. Let $\{G_1, \dots, G_n\}$ denote the resulting collection of planar graphs. The surface S_σ is a fiber if and only if for each G_i , the associated checkerboard surface is a fiber.*

Note that a spanning surface for a link in S^3 can only be a fiber if it is orientable; thus we restrict to orientable surfaces in Theorem 2.5. Observe from the definitions that a state surface will be orientable if and only if its state graph is bipartite, so we restrict to bipartite state graphs.

Remark 2.6. By Lemma 2.4, to determine if a state surface is a fiber, it suffices to collapse consecutive edges with distinct labels. But this is done in Theorem 2.5 after the state graph has been decomposed along cut-vertices and reduced. The decomposition and reduction may create new consecutive edges with distinct labels, which can then be collapsed. However, the isotopy of Lemma 2.4 does not extend in general across a cut-vertex, or across multiple crossings corresponding to parallel edges.

Corollary 2.7. *Let K_1, K_2 be diagrams of links in S^3 and let S_1, S_2 be oriented state surfaces associated to the states σ_1, σ_2 of the diagrams, respectively. Decompose the corresponding state graphs G_1, G_2 along cut-vertices into planar graphs, and for each planar graph component,*

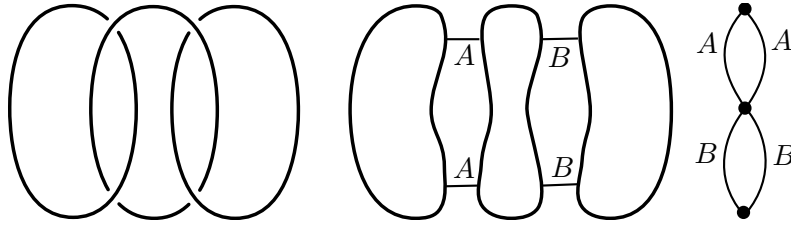


FIGURE 6. Left to right: A diagram, a Kauffman state σ determines H_σ , and the corresponding state graph. Note the state graph is isomorphic to that in figure 2.

take the associated reduced graph and remove consecutive edges with distinct labels. Suppose that the reduced planar graphs coming from G_1 can be matched in one-to-one correspondence with the reduced planar graphs coming from G_2 , by ambient isotopy within the plane via an isotopy preserving labels A and B . Then S_1 is a fiber if and only if S_2 is. \square

We illustrate Corollary 2.7 by an example. In figures 2 and 6 we have two distinct links with given resolutions, each with a single cut-vertex. When we decompose, for each link we obtain two graphs that are cycles with two edges having the same label. The reduced graphs of the decomposition are then a pair of single edges, one labeled A and one labeled B . Thus the hypotheses of Corollary 2.7 are satisfied, and one is fibered if and only if the other is fibered. In this case, both examples are well-known to be fibered. Notice, however, that the links and the state surfaces are completely different (not homeomorphic).

A Kauffman state is said to be *homogeneous* if all resolutions of the diagram in each region are the same, and *adequate* if there are no 1-edge loops. In [6] and [7], it was shown that a state surface associated with a homogeneous, adequate state is a fiber if and only if the reduced state graph is a tree. We obtain the following corollary.

Corollary 2.8. *Suppose K is a link in S^3 with oriented state surface S_σ , and suppose the associated reduced state graph G_σ is a tree. Then S_σ is a fiber.*

Proof. If the reduced state graph G_σ is a tree, it decomposes along cut-vertices into a collection of graphs made up of single edges. For each single edge, the associated checkerboard surface is the state surface of a homogeneous state, thus by [6, 7], each is fibered. Then Theorem 2.5 implies the original link is also fibered. \square

Note that Girão, Nogueira, and Salgueiro also obtained a result that a particular state surface is a fiber if and only if the associated state graph is a tree [13]. However, the converse to Corollary 2.8 is not true. There are examples of states for which the state graph is not a tree, and yet the state surface is still a fiber. We present examples below, such as Example 4.7. These contrast to the results of [6, 7, 13].

3. MURASUGI SUMS AND CUT-VERTICES

This section gives the proof of Theorem 2.5. We first recall standard definitions and results from fibered knot theory.

Definition 3.1. The oriented surface T in S^3 with boundary L is the *Murasugi sum* of the two oriented surfaces T_1 and T_2 with boundaries K_1 and K_2 if there exists a 2-sphere S in S^3 bounding balls B_1 and B_2 with $T_i \subset B_i$ for $i = 1, 2$, such that $T = T_1 \cup T_2$ and $T_1 \cap T_2 = D$, where $D \subset S$ is a $2k$ -sided polygon (a disk). See Figure 7.

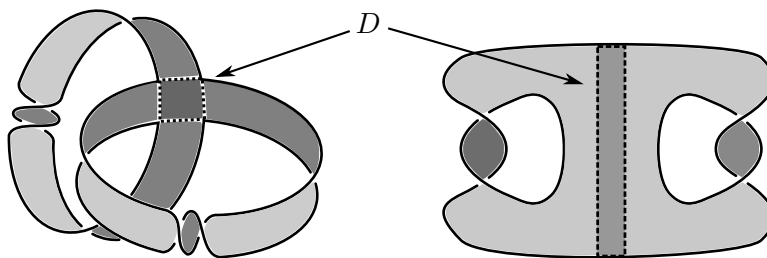


FIGURE 7. Two possible ways to obtain a surface as the Murasugi sum of two Hopf bands.

The result concerning Murasugi sum we need is the following, due to Gabai [10].

Theorem 3.2 (Gabai). *Let $T \subset S^3$, with $\partial T = K$, be a Murasugi sum of oriented surfaces $T_i \subset S^3$, with $\partial T_i = K_i$, for $i = 1, 2$. Then $S^3 - L$ is fibered with fiber T if and only if $S^3 - K_i$ is fibered with fiber T_i for $i = 1, 2$. \square*

Lemma 3.3. *Let G_σ be a state graph embedded in S^3 and suppose there is a cut-vertex v that decomposes G_σ into graphs G_1, G_2 . Consider the state surface S_i induced by σ and the subgraph G_i of G_σ , $i = 1, 2$. Then S_σ is a fiber if and only if each of S_1 and S_2 is a fiber.*

Proof. Each vertex v of G_σ is associated to a disk D in the state surface S_σ . The fact that v is a cut-vertex means that S_1 and S_2 lie in balls B_1, B_2 , with $D = S_1 \cap S_2$, as required by Definition 3.1. Thus the result follows from Theorem 3.2. \square

Theorem 3.2 gives a quick proof of the following proposition.

Proposition 3.4. *Suppose K is a link diagram with oriented state surfaces S_σ and associated state graph G_σ embedded as a spine in S_σ . Decompose the state graph G_σ along cut-vertices into planar graphs. Then S_σ is a fiber if and only if for each graph in the decomposition of G_σ the associated checkerboard surface is a fiber.*

Proof. The graph G_σ decomposes along cut-vertices into planar subgraphs $\{G_1, \dots, G_n\}$ by Lemma 2.2. By Lemma 3.3, S_σ is a fiber if and only if the state surfaces induced by the G_j are fibers. \square

3.1. Further decompositions of graphs. To go from Proposition 3.4 to Theorem 2.5, we need to consider reduced graphs. The main tool is the following lemma.

Lemma 3.5. *Suppose the state graph G_σ has a planar embedding induced from the state surface S_σ . Suppose it has multiple edges connecting a pair of vertices, and suppose that those edges are parallel (ambient isotopic) in the plane.*

- (1) *If multiple parallel edges have the same label, then S_σ is a fiber if and only if the same is true for the state surface corresponding to the graph with all but one of the edges removed.*
- (2) *If two of the parallel edges have distinct labels, then S_σ is not a fiber.*

Proof. In both cases, we may use a Murasugi sum to decompose the surface. In the first case, parallel edges with the same label correspond to a Murasugi sum of a Hopf band; see Figure 8. The twisted annulus bounded by a Hopf band is well-known to be fibered.

In the second case, parallel edges with different labels correspond to a Murasugi sum of an annulus; see Figure 9. The untwisted annulus in S^3 is well-known not to be fibered. Then the result follows by Gabai's theorem, Theorem 3.2. \square

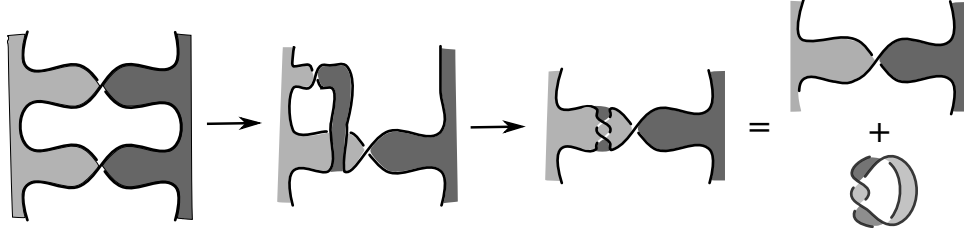


FIGURE 8. A pair of edges with the same label correspond to the decomposition of a Hopf band.

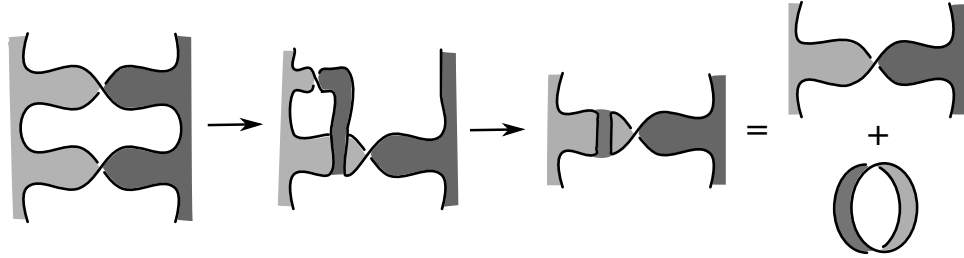


FIGURE 9. A pair of edges with distinct label correspond to the decomposition of an annulus.

Corollary 3.6. *Suppose K is a link in S^3 with oriented state surface S_σ , and suppose the associated state graph G_σ has parallel edges with distinct labels. Then S_σ is not a fiber.*

Proof. Parallel edges with distinct labels will remain parallel edges with distinct labels after decomposing along cut-vertices. Then the result follows from Theorem 2.5 and Lemma 3.5. \square

Proof of Theorem 2.5. By Proposition 3.4, S_σ is a fiber if and only if for each graph in the decomposition of its state graph along cut-vertices, the associated checkerboard surface is a fiber. By Lemma 3.5, that checkerboard surface is a fiber if and only if the checkerboard surface associated with the corresponding reduced graph is a fiber. By Lemma 2.4, the checkerboard surface associated with the reduced graph is a fiber if and only if the same is true of the checkerboard surface associated with the graph obtained by collapsing consecutive edges that do not have the same label. \square

4. STALLINGS CRITERION

By Theorem 2.5, we may reduce the task of determining which state surfaces are fibers to considering checkerboard surfaces. To determine which checkerboard surfaces are fibers, we will apply the following theorem of Stallings [30].

Theorem 4.1 (Stallings). *Let $S \subset S^3$ be a compact, connected, oriented surface with nonempty boundary ∂S . Let $S \times [-1, 1]$ be a regular neighborhood of S and let $S^+ = S \times \{1\} \subset S^3 - S$. Let $f = \varphi|_S$, where $\varphi: S \times [-1, 1] \rightarrow S^+$ is the projection map. Then S is a fiber for the link ∂S if and only if the induced map $f_*: \pi_1(S) \rightarrow \pi_1(S^3 - S)$ is an isomorphism.*

As a consequence of Theorem 4.1, we obtain a tool to determine fibering from state graphs:

Theorem 4.2. *Let S_σ be a state surface with state graph G_σ embedded as a spine, and let x be a basepoint on $G_\sigma \subset S_\sigma$. Let $f = \varphi|_S$, where $\varphi: S_\sigma \times [-1, 1] \rightarrow S_\sigma^+$ is the projection map,*

and let $y = f(x)$. Then the map f uniquely determines a map $\phi: \pi_1(G_\sigma, x) \rightarrow \pi_1(S^3 - G_\sigma, y)$, and S_σ is a fiber if and only if the map ϕ is an isomorphism of groups.

Proof. The graph G_σ lies naturally in S_σ as a spine, and therefore the inclusion $G_\sigma \rightarrow S_\sigma$ induces an isomorphism $\pi_1(G_\sigma) \rightarrow \pi_1(S_\sigma)$. Similarly, there is an isomorphism

$$\pi_1(S^3 - N(S_\sigma)) \rightarrow \pi_1(S^3 - S_\sigma)$$

induced by the deformation retraction $S^3 - S_\sigma$ to $S^3 - N(S_\sigma)$, where $N(\cdot)$ denotes a regular neighborhood. Deformation retractions (and inclusions) induce the following additional isometries:

$$\pi_1(S^3 - N(S_\sigma)) \cong \pi_1(S^3 - N(G_\sigma)) \cong \pi_1(S^3 - G_\sigma).$$

Finally note that we may also assume

$$f(S_\sigma) = S_\sigma^+ \subset S^3 - N(S_\sigma).$$

Consider the map

$$\phi: \pi_1(G_\sigma, x) \rightarrow \pi_1(S^3 - G_\sigma, y)$$

induced by the following compositions:

$$G_\sigma \rightarrow S_\sigma \rightarrow (S^3 - S_\sigma) \rightarrow (S^3 - N(S_\sigma)) \rightarrow (S^3 - N(G_\sigma)) \rightarrow (S^3 - G_\sigma),$$

where the first map is the inclusion, the second map is the map f , the third map is given by deformation retraction, and the fourth and fifth maps are given by inclusion. Thus the map ϕ is an isomorphism if and only if the map f_* in Stallings theorem is an isomorphism, and S_σ is a fiber if and only if ϕ is an isomorphism. \square

We call the map ϕ in Theorem 4.2 the *Stallings map*. We need to determine the effect of the Stallings map. We start by considering the form of the complement $S^3 - S_\sigma$.

Suppose that a state graph G_σ , embedded as the spine of a state surface S_σ , is planar with no cut-vertices. Then $S^3 - S_\sigma$ is a handlebody built as follows.

- There is one 0-handle H_+ above the plane of projection P , and one H_- below.
- For each region R_j of $P - G_\sigma$, there is a 1-handle T_j running through that region with one end on H_+ and the other on H_- .

Lemma 4.3. *Suppose that the state graph G_σ , embedded as the spine of a state surface S_σ , is planar and has no cut-vertices. Suppose that S_σ is oriented, so G_σ is bipartite, with vertices labeled $+$ and $-$, and edges labeled A and B according to the choice of resolution. Let γ be a directed arc in $G_\sigma \subset S_\sigma$ that runs over an edge. Denote the 0-handles of $S^3 - S_\sigma$ by H_+ and H_- , as above. Let T_ℓ denote the 1-handle running through the region to the left of the edge (determined by the direction of γ), and let T_r denote the 1-handle running through the region to the right. Then the effect of the map $f = \varphi|_S$, where $\varphi: S \times [-1, 1] \rightarrow S^+$ is the projection map, is as follows.*

- (1) *If γ is a monotonic arc running from a vertex labeled $+$ to one labeled $-$ over an edge labeled A , then $f(\gamma)$ runs from H_+ to H_- along the 1-handle T_ℓ .*
- (2) *If γ runs from a vertex labeled $+$ to one labeled $-$ over an edge labeled B , then $f(\gamma)$ runs from H_+ to H_- along the 1-handle T_r .*
- (3) *If γ runs from a vertex labeled $-$ to one labeled $+$ over an edge labeled A , then $f(\gamma)$ runs from H_- to H_+ along the 1-handle T_r .*
- (4) *If γ runs from a vertex labeled $-$ to one labeled $+$ over an edge labeled B , then $f(\gamma)$ runs from H_- to H_+ along the 1-handle T_ℓ .*

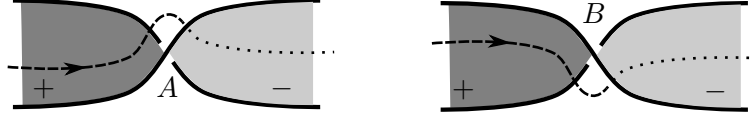


FIGURE 10. Effect of the map f on the edges of G_σ for γ running from $+$ to $-$. For $-$ to $+$, simply change the direction γ .

Proof. If γ starts on a vertex labeled $+$ and runs to one labeled $-$, then $f(\gamma)$ begins at H_+ and ends at H_- . Similarly if γ starts at a vertex labeled $-$ and runs to one labeled $+$, then $f(\gamma)$ begins at H_- and ends at H_+ . The 1-handles that $f(\gamma)$ meets are determined by the twisting of S_σ along the twisted band attached at the crossing of the edge, with twisting in one direction for an edge labeled A and in the other direction for an edge labeled B . The effects are shown in Figure 10. \square

Suppose G_σ is a state graph that comes out of Theorem 2.5, namely it is planar with no cut-vertices. To determine whether the associated state surface S_σ is a fiber, we choose generators for $\pi_1(G_\sigma, x)$ and consider their image under the Stallings map ϕ .

Because S_σ is orientable, G_σ is bipartite, i.e. every closed loop has even length. Label each vertex either by $+$ or $-$ in an alternating fashion. Label the basepoint x in G_σ with $+$ to obtain a well-defined labeling of vertices of G_σ .

The graph G_σ divides the plane into regions. The unbounded region is denoted by R_0 . The bounded ones are denoted by R_1, \dots, R_n .

Corresponding to each region R_j , there is a 1-handle T_j with its ends on the 0-handles H_+ and H_- , above and below the plane of projection, respectively. Since the basepoint x of G_σ is labeled $+$, its image $y = f(x)$ lies on H_+ . For each bounded region R_j , $j = 1, \dots, n$, define a curve u_j based at y as follows. The curve u_j leaves the basepoint y and runs monotonically down the 1-handle T_j through the region R_j to the 0-handle H_- . It then runs up the 1-handle T_0 through the unbounded region to connect to H_+ , and back to the basepoint y . Then $\{u_1, \dots, u_n\}$ form a generating set for $\pi_1(S^3 - G_\sigma, x)$.

Given a loop $u \subset S^3 - G_\sigma$ based at y , its homotopy class in $\pi_1(S^3 - G_\sigma, y)$ is given by a word in the letters u_1, \dots, u_n as follows: Starting at y , move along u according to the choice of orientation. If u crosses a region R_i from above to below, then write the letter u_i . If u crosses a region R_i from below to above, then write the letter u_i^{-1} . Going around u once gives a word which represents its homotopy class in $\pi_1(S^3 - G_\sigma, y)$. If the region R_0 is crossed, then write no letters.

Definition 4.4. The following procedure defines a new labeling on the graph G_σ , with labels the letters u_i . Direct each edge from $+$ to $-$. If the edge is labeled A , assign to the directed edge the letter u_i , where R_i is the region to the left of the directed edge, or 1 if the region to the left is unbounded. If the edge is labeled B , assign the letter u_j , where R_j is the region to the right of the directed edge, or 1 if the region to the right is unbounded.

Proposition 4.5. *Suppose that the state graph G_σ , embedded as the spine of an oriented state surface S_σ , is planar and has no cut-vertices. The effect of the Stallings map $\phi: \pi_1(G_\sigma, x) \rightarrow \pi_1(S^3 - G_\sigma, y)$ is as follows. A generator γ_i of $\pi_1(G_\sigma, x)$ is represented by a word in the edges of G_σ . The image of γ_i under ϕ is represented by a word in the letters $\{u_1^{\pm 1}, \dots, u_n^{\pm 1}\}$, where each edge e contributes a letter as follows.*

Consider the labeling of Definition 4.4.

- (1) If u_j is the label on e , and γ_i runs along e from $+$ to $-$, write u_j .

- (2) If u_j is the label on e , and γ_i runs along e from $-$ to $+$, write u_j^{-1} .
- (3) If e is labeled 1 and γ_i runs along e , write no letters.

Proof. This follows from Lemma 4.3 and our choice of generators of $\pi_1(G_\sigma, x)$ and $\pi_1(S^3 - G_\sigma, y)$ defined above. \square

Corollary 4.6. *Suppose that the state graph G_σ , embedded in the spine of an oriented state surface S_σ , is planar with no cut-vertices, and let $\gamma_1, \dots, \gamma_n$ denote the generators of $\pi_1(G_\sigma, x)$ as above. Then S_σ is a fiber if and only if the group generated by $\phi(\gamma_1), \dots, \phi(\gamma_n)$ is isomorphic to $\pi_1(S^3 - G_\sigma, y)$.* \square

Example 4.7. Consider the link in Figure 11. The base point x is indicated. The labeling

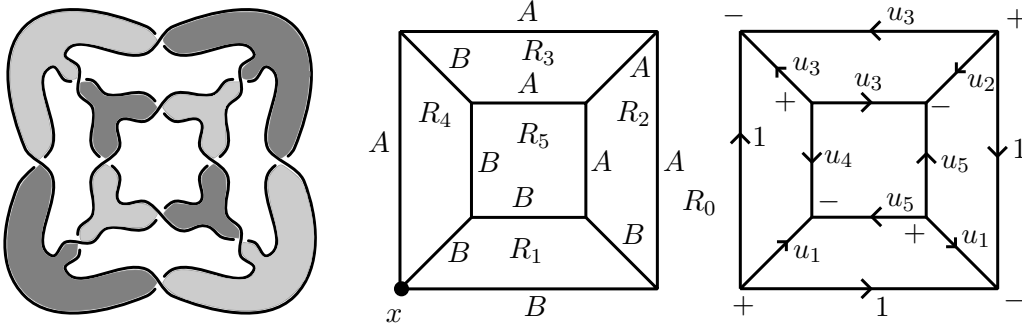


FIGURE 11. A checkerboard state surface that is a fiber, and its associated state graph.

of Definition 4.4 is shown on the far right. Let $\{\gamma_1, \dots, \gamma_5\}$ denote generators of $\pi_1(G_\sigma, x)$ as follows. The curve γ_i begins at x , traverse a path β_i to the boundary of the region R_i , runs counter clockwise around R_i , then traverses the path β_i^{-1} back to x . More specifically, we choose β_2 to be the arc given by the lower horizontal edge starting at x , we choose β_3 to be the arc given by the lower horizontal edge followed by the vertical right-most edge, and we choose β_5 to be the diagonal edge with endpoint on x . The arcs β_1 and β_4 are trivial. Following the recipe of Proposition 4.5, we obtain:

$$\begin{cases} \phi(\gamma_1) = u_1^{-1}u_5u_1^{-1} \\ \phi(\gamma_2) = u_2u_5^{-1}u_1 \\ \phi(\gamma_3) = u_3u_2^{-1} \\ \phi(\gamma_4) = u_1u_4^{-1}u_3 \\ \phi(\gamma_5) = u_1u_3^{-1}u_4u_1^{-1} \end{cases}$$

It is possible to see directly that this map is an isomorphism; its inverse given by:

$$\begin{cases} \phi^{-1}(u_1) = \gamma_5\gamma_4 \\ \phi^{-1}(u_2) = \gamma_2\gamma_1\gamma_5\gamma_4 \\ \phi^{-1}(u_3) = \gamma_3\gamma_2\gamma_1\gamma_5\gamma_4 \\ \phi^{-1}(u_4) = \gamma_3\gamma_2\gamma_1\gamma_5^2\gamma_4 \\ \phi^{-1}(u_5) = \gamma_5\gamma_4\gamma_1\gamma_5\gamma_4 \end{cases}$$

Therefore the state surface shown is a fiber for the corresponding link.

4.1. Stallings folding. In [31], Stallings describes a procedure that can determine whether a homomorphism of free groups is an isomorphism. See also Kapovich and Myasnikov [20].

Definition 4.8. An *edge folding* of a directed labeled graph Γ is a new directed labeled graph obtained by identifying two edges e_1 and e_2 of Γ that share the same vertex v , and have the same label and the same direction incident to v . A directed labeled graph is *folded* if at each vertex v there is at most one edge with a given label and incidence starting (or terminating) at v .

A folded graph admits no edge foldings.

Fix a basepoint on a directed labeled graph. The fundamental group of the graph is determined by concatenation of paths; group elements are determined by writing words in the labels traversed by a path, where if an edge e has label a and is traversed in the direction of e , we write a , and if in the opposite direction, we write a^{-1} . Two words are *freely reduced* if two labels a and a^{-1} never appear consecutively. Note this is a way of representing the fundamental group as a subgroup of a free group; the labeled graph is a covering space corresponding to the subgroup. We call this the *group defined on the graph*.

The following is straightforward; see [20].

Proposition 4.9. *Let Γ_1 and Γ_2 be two directed labeled graphs. If Γ_2 is obtained from Γ_1 by an edge folding, then the two groups defined on the graphs are isomorphic. If Γ_2 is folded, then for any loop ℓ in Γ_2 , the corresponding word is freely reduced.*

Starting with any graph, perform a sequence of edge foldings, strictly reducing the number of edges, until the process terminates in a folded graph. Touikan showed that there is an algorithm to fold a graph that runs in almost linear time [32].

Corollary 4.10. *Suppose G_σ is a planar state graph with no cut vertices that is embedded as the spine of an oriented state surface S_σ . Suppose $\pi_1(G_\sigma)$ is the free group on n letters. Let Γ be a directed labeled graph obtained from G_σ by the process of Definition 4.4. Let Γ' denote the result of Γ after folding. Then the state surface S_σ is a fiber if and only if Γ' is a rose with n petals.*

Proof. The graph Γ encodes the image of Stallings' map $\phi: \pi_1(G_\sigma) \rightarrow \pi_1(S^3 - G_\sigma)$. Stallings folding implies that the graph Γ' is a rose with n petals if and only if ϕ is surjective. Because free groups are Hopfian, this holds if and only if ϕ is an isomorphism. The result follows from Theorem 4.2. \square

Figure 12 shows the folding process applied to the directed labeled graph of Figure 11. Note the fact that the state surface of that example is a fiber now follows from Corollary 4.10.

5. APPLICATIONS

In this section, we consider some simple graphs and completely classify when they correspond to state surfaces that are fibers.

5.1. The state graph or reduced state graph is a tree. This is the case of Corollary 2.8. We have seen that the state surface is always a fiber.

5.2. The reduced state graph decomposes into cycles.

Lemma 5.1. *Suppose K is a link with state surface S_σ . Suppose that the reduced state graph corresponding to S_σ is a cycle. Then S_σ is a fiber if and only if there are exactly two more edges in the cycle labeled A than B , or vice versa.*

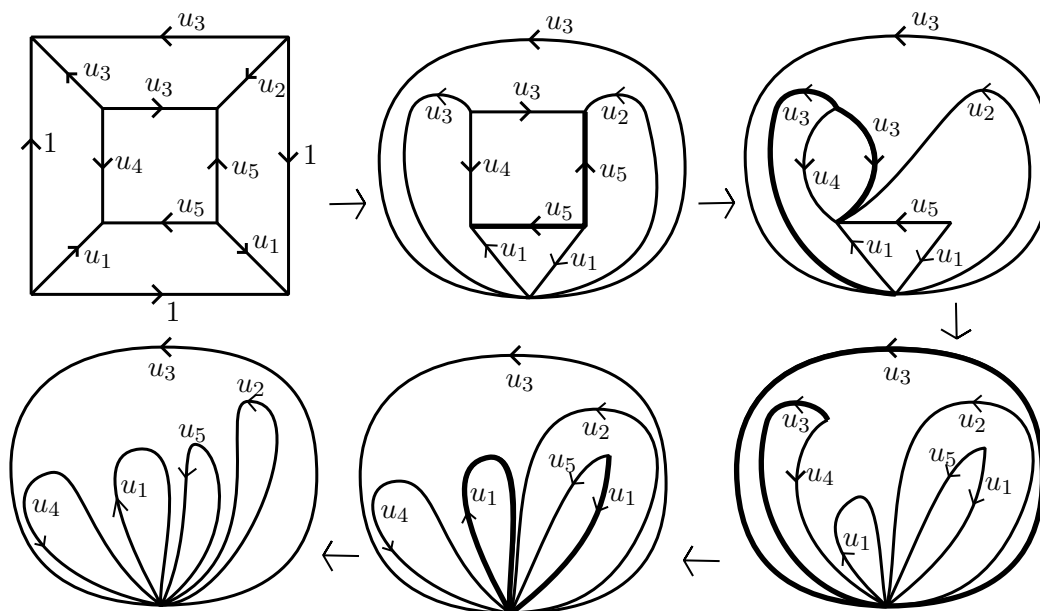


FIGURE 12. The process of folding applied to Example 4.7.

Proof. Let G denote the reduced state graph; the fact that G is a cycle means that the (checkerboard) state surface S induced by G is an annulus. The original state surface S_σ , whose state graph may have multiple parallel edges with the same label, is obtained by taking Murasugi sums of Hopf bands with the annulus S , as in Lemma 3.5. The graph G is a string of consecutive edges. Untwist S as in Lemma 2.4, obtaining a new graph G' for which all edges have the same label. Now consider the Stallings map ϕ . Because the surface is orientable, G' has an even number of edges. We have $\pi_1(G) \cong \pi_1(G') \cong \mathbb{Z}$ and $\pi_1(S^3 - G) \cong \pi_1(S^3 - G') \cong \mathbb{Z}$. By Proposition 4.5, the image of the generator under ϕ is given by $\phi(\gamma) = u^{\pm r}$, where $2r$ is the number of edges in G' , and the sign is positive or negative depending on whether the labels of G' are A or B . Note ϕ is an isomorphism if and only if $r = 1$. Thus the original state surface is a fiber in this case if and only if G' has exactly two edges, meaning there are exactly two more edges of the reduced graph G that are labeled A than those labeled B , or vice versa. \square

Note that the unbounded checkerboard surfaces for pretzel links fall into the class of the surfaces satisfying the hypotheses of Lemma 5.1. Gabai treats these as type III surfaces in [10]. Gabai has more conditions on when these links fiber. However, note that in the cases distinct from Lemma 5.1, the fibered surface is not the given state surface.

5.3. Graphs the shape of a theta and pretzel links. A next simple class of graphs to consider are those that have the shape of a Θ : that is, there are three collections of consecutive edges meeting two vertices; we call each of the three collections of consecutive edges a *strand*. There will be p_1 vertices on the first strand, p_2 on the second, and p_3 on the third, where either all p_i are even or all are odd to ensure the graph is bipartite. We may also assume, after reducing, that all edges on each strand have the same label. The induced checkerboard state surface will be the bounded checkerboard surface of a pretzel knot with three strands, and p_i crossings on each strand. In fact we may generalize to n strands: each strand has p_i vertices, all edges on a strand have the same label, and all the p_i are even or all are odd.

Call such a graph a *generalized theta graph*. The induced checkerboard surfaces are bounded checkerboard surfaces for pretzel links.

The fibering of such checkerboard surfaces has been completely classified. When $n = 3$, this follows from work of Crowell and Trotter [3]. For other values of n , partial results were obtained by Parris [28], and independently by Goodman and Tavares [14], and Kanenobu [19]. Their results are summarized and generalized by Gabai [10]. The full result is the following.

Theorem 5.2 (Bounded checkerboard surfaces of pretzel links). *Let p_1, \dots, p_n be nonzero integers. The pretzel link determined by (p_1, \dots, p_n) crossings has a bounded checkerboard surface that is a fiber if and only if one of the following holds:*

- (1) *each $p_i = \pm 1$ or ∓ 3 and some $p_i = \pm 1$.*
- (2) *$(p_1, \dots, p_n) = \pm(2, -2, 2, -2, \dots, 2, -2, \ell)$ for $\ell \in \mathbb{Z}$ (here n is odd).*
- (3) *$(p_1, \dots, p_n) = \pm(2, -2, 2, -2, \dots, -2, 2, -4)$ (here n is even).*

Corollary 5.3. *Suppose a reduced state graph has the shape of a generalized theta graph. Reduce further to remove consecutive edges without the same label. Then the associated checkerboard surface is a fiber if and only if one of the following holds:*

- (1) *Each strand has 0 or 2 vertices, and some strand has 0 vertices. All strands with 0 vertices are labeled A or are all labeled B; strands with 2 vertices are exactly the opposite (all B or all A).*
- (2) *There are an even number of strands, each strand except the last has 1 vertex, all strands except the last alternate being labeled A and B, and the final strand has any number of vertices with any label A or B on all edges of the strand.*
- (3) *There are an odd number of strands, each strand except the last has 1 vertex, all strands alternate being labeled A and B, and the final strand has three vertices.*

5.4. Checkerboard surfaces of two-bridge links. We conclude with one final family of reduced state graphs whose fibering we can completely classify: those that arise from diagrams of 2-bridge knots. Essential surfaces in 2-bridge knots were classified by Hatcher and Thurston [16], and they note in that paper that those spanning surfaces that are fibers are exactly those that embed in a diagram $K[a_{n-1}, \dots, a_1]$ with each $a_j = \pm 2$ (notation described below). However, the surfaces in [16] are not isotoped to be checkerboard surfaces. While essential checkerboard surfaces must appear in their theorem, a nontrivial isotopy of the entire link is required move a standard checkerboard surface into one of the forms of their results. Since state graphs induce diagrams and checkerboard surfaces, we are interested in classifying those that lead to fibered surfaces without having to isotope into a form required by [16].

In this section, we classify all state graphs corresponding to 2-bridge knots and links that induce checkerboard surfaces that are fibers. Note that while the surfaces must be isotopic to one in $K[\pm 2, \dots, \pm 2]$ as in [16], the diagrams we obtain here are much broader.

We begin by recalling results and notation. Recall that *2-bridge knot* or link is obtained by taking the closure of a rational tangle, determined by a rational number p/q ; see for example [23]. For any continued fraction

$$\frac{p}{q} = [a_n, a_{n-1}, \dots, a_1] = a_n + \frac{1}{a_{n-1} + \frac{1}{\ddots + \frac{1}{a_1}}}$$

we obtain a diagram of the knot with $(n - 1)$ twist regions, with $|a_i|$ crossings in the i -th twist region, and with signs of the crossings equal to the sign of a_i if i is even, and $-a_i$ if i is odd.

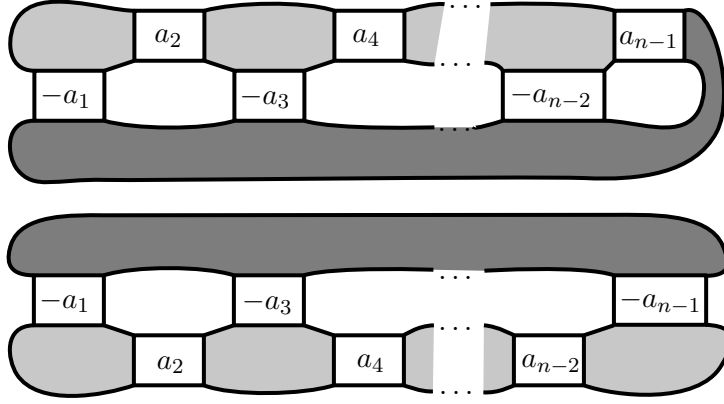


FIGURE 13. The diagram of $K[a_{n-1}, \dots, a_1]$. Top: n odd; bottom: n even. Box labeled $\pm a_i$ denotes a (horizontal) twist region with $|a_i|$ crossings, with sign of the crossings equal to that of $\pm a_i$.

Denote this diagram by $K[a_{n-1}, \dots, a_1]$. See Figure 13. Note that the value of a_n does not affect the knot, and it can be removed from the diagram, so we omit it from the notation. Note also that we may assume $|a_i| \geq 0$, since diagrams with 0 crossings in a twist region may be described instead by fewer twist regions, with crossings above and below merged. Similarly we may assume $|a_1| \geq 2$ and $|a_{n-1}| \geq 2$.

Associated with each such diagram are two checkerboard surfaces. We will be interested in the bounded checkerboard surface, as shown in Figure 13.

Now consider the state graph of this checkerboard surface. There will be one vertex corresponding to the large disk in the diagram, which we will label $+$ and denote as the basepoint. For each odd a_{2j+1} , the basepoint will be adjacent to $b_{2j+1} = |a_{2j+1}|$ parallel multi-edges, with each edge labeled A if $a_{2j+1} > 0$ and B otherwise. The opposite endpoint of the b_{2j+1} edges will be connected to the endpoint of the b_{2j-1} edges via a strand of $b_{2j} = |a_{2j}|$ consecutive edges, all labeled A if $a_{2j} > 0$ and B otherwise. If $n = 2k + 3$ is odd, the basepoint is also connected to the other endpoint of the b_{2k+1} multi-edges by a sequence of $|a_{2k+2}| := b_{2k+2}$ consecutive edges, labeled A if $a_{2k+1} > 0$ and B otherwise. See Figure 14, left. The reduced state graph replaces each group of b_{2j-1} parallel multi-edges with a single edge, denoted e_j . See Figure 14, right. By Lemma 3.5, the checkerboard surface is a fiber if and only if the induced checkerboard surface of the reduced graph is a fiber.

Since we only consider orientable surfaces, we must have b_{2j} even, for $j = 1, \dots, k$. If n is odd, then b_{2k+2} must also be odd, else we cannot label the vertices $+$ and $-$ in an alternating manner. Replace the b_{2k+2} edges in this case by one edge e_{k+2} , and by $b_{2k+2} - 1$ additional edges with the same label, where $b_{2k+2} - 1$ is even. Then the form of the reduced graph in the even and odd cases agree, so we can apply a single argument to both. Namely, there are regions R_0 (unbounded), R_1, \dots, R_k (or R_{k+1}), with R_j bordered by edges e_j, e_{j+1} , and a collection of b_{2j} consecutive edges, which we will denote by the strand ϵ_j .

We may assume that the edge e_1 in G'_σ has the same label as the other b_2 edges in the boundary of R_1 , or else we may remove two crossings, as in Lemma 2.4. Similarly, in the case $n = 2k + 3$ is odd, the edge e_{k+1} has the same label as the other b_{2k} edges in the region R_k .

We now consider generators of the fundamental group $\pi_1(G'_\sigma)$. First we set as basepoint the vertex x on the left of the reduced graph G'_σ . The generators of $\pi_1(G'_\sigma)$ are $\{\gamma_1, \dots, \gamma_k\}$ (or $\{\gamma_1, \dots, \gamma_{k+1}\}$), where γ_j corresponds to the oriented boundary of the region R_j , oriented

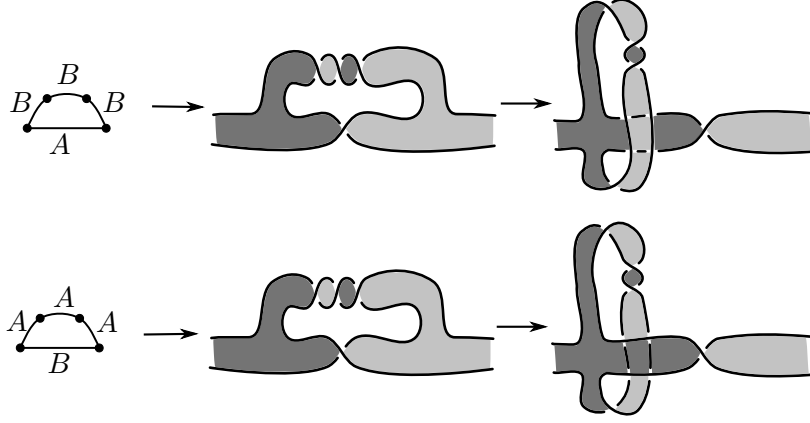


FIGURE 15. Top: Part (b) of Case I; Bottom: Part (a) of Case II.

and its determinant is given by

$$\det(M) = \prod_{i=1}^m p_i.$$

Notation in the lemma: $m = k$ when $n = 2k + 2$ is even, and $m = k + 1$ when $n = 2k + 3$ is odd.

Proof. The fact that the induced map on homology is tridiagonal follows immediately from Lemma 5.4: each word $\phi(\gamma_j)$ involves at most the generators u_{j-1} , u_j , and u_{j+1} .

The terms of the matrix are integers that encode the powers of the generators u_i . Note that since the region R_j shares a single edge with each of its neighboring regions, it must be the case that $|q_j| + |r_j| = 1$. Thus the determinant of M is $\prod_{i=1}^n p_i$. \square

Lemma 5.6. *Let $K[a_n, a_{n-1}, \dots, a_1]$ be a 2-bridge link with bounded checkerboard surface S_σ . Let M denote the matrix of Lemma 5.5. Then S_σ is a fiber if and only if $|\det(M)| = 1$.*

Proof. By Theorem 4.2 and Lemma 3.5, S_σ is a fiber if and only if the Stallings map $\phi': \pi_1(G'_\sigma) \rightarrow \pi_1(S^3 - G'_\sigma)$ is an isomorphism.

If ϕ' is an isomorphism, then it must be the case that $\det(M) = \pm 1$.

We show the converse: if $\det(M) = \pm 1$ then ϕ' is an isomorphism. In fact, if $\det(M) = \pm 1$, then $|p_i| = 1$, for $i = 1, \dots, n$. We proceed by induction on the regions R_1, \dots, R_m .

Recall that the b_i are even, positive integers.

Case I: If e_2 is labeled A , there are two possibilities for $\phi'(\gamma_1)$:

- (a) $\gamma_1 \mapsto u_1 u_1^{b_2/2} = u_1^{b_2/2+1}$, if e_1 and the other edges of R_1 are labeled A , or
- (b) $\gamma_1 \mapsto u_1 u_1^{-b_2/2-1} = u_1^{-b_2/2}$, if e_1 and the other edges of R_1 are labeled B .

Since $|p_1| = 1$, if (a) happens, we must have $b_2 = 0$, which we ruled out by our choices. If (b) happens, we must have $b_2 = 2$. In this case we are able to decompose a Hopf band. The decomposition of case (b) is illustrated in Figure 15 (top).

Case II: If e_2 is labeled B , again there two possibilities for $\phi'(\gamma_1)$:

- (a) $\gamma_1 \mapsto u_2 u_1^{b_2/2}$, if e_1 and the other edges of R_1 are labeled A ,
- (b) $\gamma_1 \mapsto u_2 u_1^{-b_2/2-1}$, if e_1 and the other edges of R_1 are labeled B .

The argument is similar to the previous case: Since $|p_1| = 1$, if (b) happens we must have $b_2 = 0$, which is impossible. If (a) happens we must have $b_2 = 2$, and we decompose a Hopf band. In (a) this decomposition is illustrated in Figure 15 (bottom).

After these decompositions we are left with a graph consisting of the regions R_2, \dots, R_n . We proceed inductively, as before, in the edges of the boundary of each region. In each step we use the fact that $|p_i| = 1$ to obtain the desired decompositions. We conclude that if $|\det(M)| = 1$ then the surface S_σ must be a fiber. \square

Theorem 5.7. *Suppose K is a 2-bridge link with diagram $K[a_{n-1}, \dots, a_1]$, where $|a_{n-1}|, |a_1| \geq 2$, and $|a_j| \geq 1$ for all j . Then the associated bounded checkerboard surface is a fiber if and only if the a_i satisfy the following.*

- (1) For odd indices $2j + 1 \neq n - 2$, a_{2j+1} can be any nonzero integer.
- (2) For even indices $2j$ with $2j < n - 1$:
 - If $a_{2j-1} > 0$ and $a_{2j+1} > 0$, then $a_{2j} = -4$.
 - If $a_{2j-1} > 0$ and $a_{2j+1} < 0$, then $a_{2j} = \pm 2$.
 - If $a_{2j-1} < 0$ and $a_{2j+1} > 0$, then $a_{2j} = \pm 2$.
 - If $a_{2j-1} < 0$ and $a_{2j+1} < 0$, then $a_{2j} = 4$.
- (3) If $(n - 1) = 2k + 2$ is even, then either $a_{2k+1} > 0$ and $a_{2k+2} = -3$, or $a_{2k+1} < 0$ and $a_{2k+2} = 3$.

Proof. By Lemma 5.6, it suffices to find all choices of the a_k for which the tridiagonal matrix of Lemma 5.5 has determinant ± 1 . To do so, we consider the images of the generators γ_j as in Lemma 5.4. For each generator, aside from the first and the last, there are eight choices of labels A and B for the edges meeting γ_j , each determining an integer p_j . When we set the p_j to be ± 1 we obtain the result.

For example, when e_j, ϵ_j and e_{j+1} are all of type A , meaning a_{2j-1}, a_{2j} , and a_{2j+1} are positive, we obtain $p_j = b_{2j}/2 + 1$. If this is $+1$, then $b_{2j} = |a_{2j}|$ must be zero, which is ruled out by our assumptions on a_{2j} . If it is -1 , then $b_{2j} = |a_{2j}| = -4$, which is impossible. So a_{2j-1}, a_{2j} , and a_{2j+1} cannot all be positive. If a_{2j-1} and a_{2j+1} are positive (type A) and a_{2j} is negative (type B), then $p_j = -b_{2j}/2 + 1$. This cannot be $+1$ by our assumption that $b_{2j} = |a_{2j}| > 0$, hence it equals -1 and $b_{2j} = 4$. The other cases are dealt with similarly.

Finally, when $(n - 1) = 2k + 2$ is even, the value of p_{k+1} depends on the signs of a_{2k+1} and a_{2k+2} . When they are both positive or both negative, we find that $p_{k+1} = \pm((b_{2k+2} - 1)/2 + 1)$, which is ± 1 only if $b_{2k+2} = |a_{2k+2}| = 1$. This is ruled out by our assumption that $|a_{n-1}| = |a_{2k+2}| \geq 2$. When $a_{2k+1} > 0$ and $a_{2k+2} < 0$, $p_{k+1} = -(b_{2k+2} - 1)/2$, which is -1 when $b_{2k+2} = |a_{2k+2}| = 3$. Similarly for $a_{2k+1} < 0$ and $a_{2k+2} > 0$. \square

REFERENCES

1. Paige Bartholomew, Shane McQuarrie, Jessica S. Purcell, and Kai Weser, *Volume and geometry of homogeneously adequate knots*, J. Knot Theory Ramifications **24** (2015), no. 8, 1550044, 29. 1
2. Stephan D. Burton and Efstratia Kalfagianni, *Geometric estimates from spanning surfaces*, Bull. Lond. Math. Soc. **49** (2017), no. 4, 694–708. 1
3. R. H. Crowell and H. F. Trotter, *A class of pretzel knots*, Duke Math. J. **30** (1963), 373–377. 14
4. Oliver T. Dasbach, David Futer, Efstratia Kalfagianni, Xiao-Song Lin, and Neal W. Stoltzfus, *The Jones polynomial and graphs on surfaces*, J. Combin. Theory Ser. B **98** (2008), no. 2, 384–399. 1

5. Kathleen Finlinson and Jessica S. Purcell, *Volumes of Montesinos links*, Pacific J. Math. **282** (2016), no. 1, 63–105. 1
6. David Futer, *Fiber detection for state surfaces*, Algebr. Geom. Topol. **13** (2013), no. 5, 2799–2807. 1, 2, 6
7. David Futer, Efstratia Kalfagianni, and Jessica Purcell, *Guts of surfaces and the colored Jones polynomial*, Lecture Notes in Mathematics, vol. 2069, Springer, Heidelberg, 2013. 1, 2, 6
8. David Futer, Efstratia Kalfagianni, and Jessica S. Purcell, *Quasifuchsian state surfaces*, Trans. Amer. Math. Soc. **366** (2014), no. 8, 4323–4343. 1
9. ———, *Hyperbolic semi-adequate links*, Comm. Anal. Geom. **23** (2015), no. 5, 993–1030. 1
10. David Gabai, *Detecting fibred links in S^3* , Comment. Math. Helv. **61** (1986), no. 4, 519–555. 1, 2, 7, 13, 14
11. Paolo Ghiggini, *Knot Floer homology detects genus-one fibred knots*, Amer. J. Math. **130** (2008), no. 5, 1151–1169. 1
12. Darlan Girão, *On the fibration of augmented link complements*, Geom. Dedicata **168** (2014), 207–220. 1, 2
13. Darlan Girão, João Nogueira, and António Salgueiro, *Fiber surfaces from alternating states*, Algebr. Geom. Topol. **15** (2015), no. 5, 2805–2817. 1, 2, 6
14. Sue Goodman and Geovan Tavares, *Pretzel-fibered links*, Bol. Soc. Brasil. Mat. **15** (1984), no. 1-2, 85–96. 14
15. John Harer, *How to construct all fibered knots and links*, Topology **21** (1982), no. 3, 263–280. 1
16. A. Hatcher and W. Thurston, *Incompressible surfaces in 2-bridge knot complements*, Invent. Math. **79** (1985), no. 2, 225–246. 2, 14
17. Mikami Hirasawa and Kunio Murasugi, *Genera and fibredness of Montesinos knots*, Pacific J. Math. **225** (2006), no. 1, 53–83. 2
18. Efstratia Kalfagianni and Christine Ruey Shan Lee, *On the degree of the colored Jones polynomial*, Acta Math. Vietnam. **39** (2014), no. 4, 549–560. 1
19. Taizo Kanenobu, *The augmentation subgroup of a pretzel link*, Math. Sem. Notes Kobe Univ. **7** (1979), no. 2, 363–384. 14
20. Ilya Kapovich and Alexei Myasnikov, *Stallings foldings and subgroups of free groups*, J. Algebra **248** (2002), no. 2, 608–668. 12
21. Louis H. Kauffman, *State models and the Jones polynomial*, Topology **26** (1987), no. 3, 395–407. 1
22. Kunio Murasugi, *On a certain subgroup of the group of an alternating link*, Amer. J. Math. **85** (1963), 544–550. 1
23. ———, *Knot theory & its applications*, Modern Birkhäuser Classics, Birkhäuser Boston, Inc., Boston, MA, 2008, Translated from the 1993 Japanese original by Bohdan Kurpita, Reprint of the 1996 translation [MR1391727]. 14
24. Lee Neuwirth, *KNOT GROUPS*, ProQuest LLC, Ann Arbor, MI, 1959, Thesis (Ph.D.)–Princeton University. 1
25. Yi Ni, *Knot Floer homology detects fibred knots*, Invent. Math. **170** (2007), no. 3, 577–608. 1
26. Makoto Ozawa, *Essential state surfaces for knots and links*, J. Aust. Math. Soc. **91** (2011), no. 3, 391–404. 1
27. Milena D. Pabiniak, Józef H. Przytycki, and Radmila Sazdanović, *On the first group of the chromatic cohomology of graphs*, Geom. Dedicata **140** (2009), 19–48. 1

28. Richard Lee Parris, *PRETZEL KNOTS*, ProQuest LLC, Ann Arbor, MI, 1978, Thesis (Ph.D.)—Princeton University. 14
29. John Stallings, *On fibering certain 3-manifolds*, Topology of 3-manifolds and related topics (Proc. The Univ. of Georgia Institute, 1961), Prentice-Hall, Englewood Cliffs, N.J., 1962, pp. 95–100. 1
30. John R. Stallings, *Constructions of fibred knots and links*, Algebraic and geometric topology (Proc. Sympos. Pure Math., Stanford Univ., Stanford, Calif., 1976), Part 2, Proc. Sympos. Pure Math., XXXII, Amer. Math. Soc., Providence, R.I., 1978, pp. 55–60. 1, 8
31. ———, *Topology of finite graphs*, Invent. Math. **71** (1983), no. 3, 551–565. 2, 12
32. Nicholas W. M. Touikan, *A fast algorithm for Stallings' folding process*, Internat. J. Algebra Comput. **16** (2006), no. 6, 1031–1045. 2, 12